iScience

CellPress
OPEN ACCESS

Article

KRT19 is regulated by miR-642a-5p and promotes pancreatic cancer progression through the Wnt/β-catenin pathway

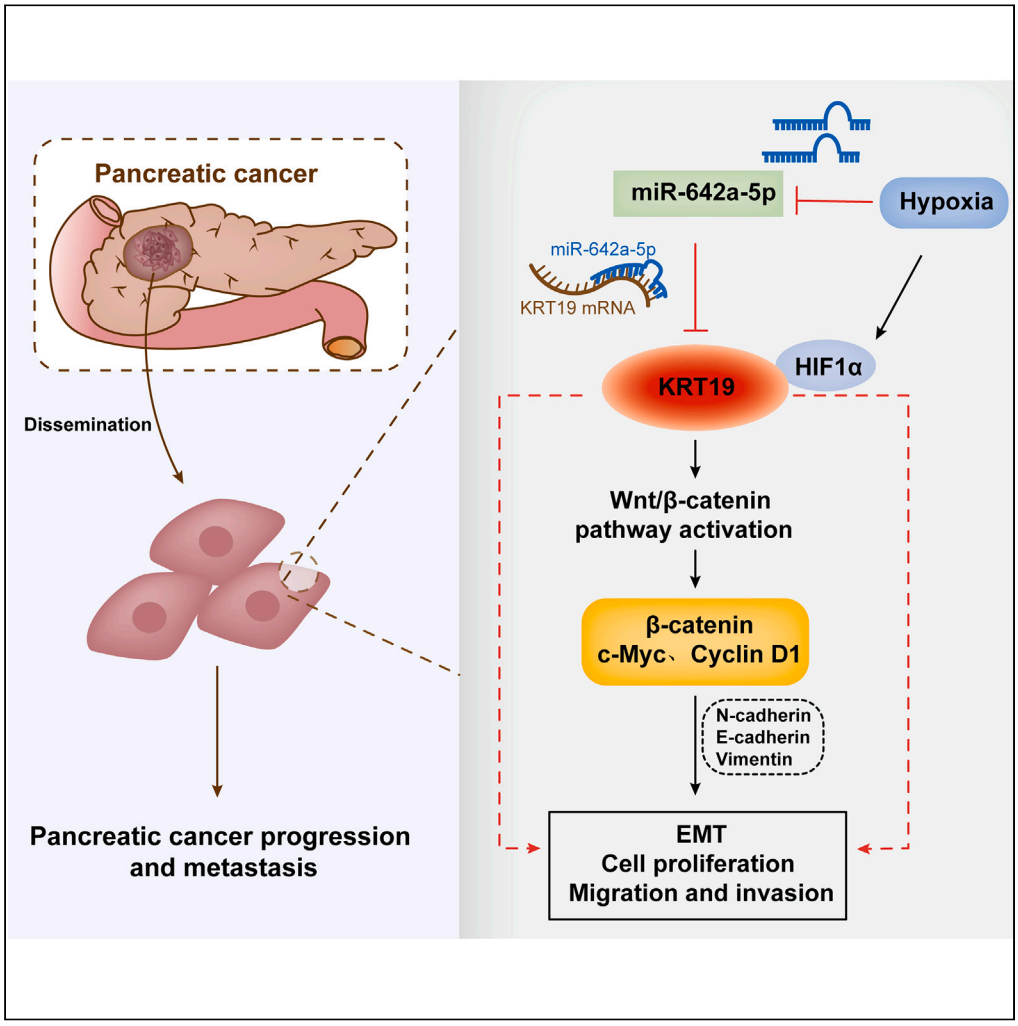

Hua-Qing Shi, Xin Li, Zhou Chen, ..., Dong-Ao Fan, Hui Zhang, Wen-Ce Zhou

ery_huizhang@lzu.edu.cn (H.Z.)
zhouwc129@163.com (W.-C.Z.)

Highlights

KRT19 is oncogenic in pancreatic cancer

KRT19 is regulated by miR-642a-5p

KRT19 regulates the Wnt/β-catenin pathway

Hypoxia promotes malignant progression of pancreatic cancer

Shi et al., iScience 27, 110782
September 20, 2024
https://doi.org/10.1016/j.isci.2024.110782

iScience

CellPress
OPEN ACCESS

Article

KRT19 is regulated by miR-642a-5p and promotes pancreatic cancer progression through the Wnt/β-catenin pathway

Hua-Qing Shi,[1,6] Xin Li,[1,3,6] Zhou Chen,[2] Shi Dong,[1] Cheng Ye,[2] Shuang Hou,[1] Dong-Ao Fan,[1] Hui Zhang,[1,3,*] and Wen-Ce Zhou[1,3,4,5,7,*]

SUMMARY

Pancreatic cancer (PC) has a really poor prognosis, and we urgently need to delve deeper into its molecular mechanisms. In this study, we found that KRT19 expression was significantly increased in PC tissues and cell lines and it was linked to unfavorable outcomes for patients. Overexpression of KRT19 boosted the proliferation, migration, and invasion of PC cells. Additionally, miR-374b-5p targets KRT19, inhibiting the activation of the Wnt/β-catenin pathway (WBC), which in turn suppresses epithelial-to-mesenchymal transition (EMT) and the progression of PC. Further experiments showed that under hypoxic conditions, HIF1α was positively correlated with KRT19, promoting its expression. The loss of miR-642a-5p and the upregulation of KRT19 induced by hypoxia can significantly favor PC progression. Plus, the increased expression of KRT19 might act as a predictive marker and potential target for PC treatment.

INTRODUCTION

Pancreatic cancer (PC) is an aggressive malignancy that affects the digestive system. PC is the seventh leading cause of cancer-related fatalities worldwide, affecting both males and females.[1] Despite the increasing number of novel PC treatments, such as nanomedicine-targeted treatment and immunotherapy, the prognosis of patients with PC remains unfavorable, particularly for those with advanced PC.[2,3] Therefore, conducting additional research on the fundamental molecular mechanisms that drive PC progression and metastasis to identify new therapeutic targets for cancer management is essential.

The role of keratin in cancer development has been increasingly studied. Berens et al. reported that the aberrant expression of associated keratins is essential for carcinogenesis.[4] In the present study, we examined the role of *KRT19*, a member of the keratin family that encodes cytoskeletal intermediate filament proteins, in PC. *KRT19* is epithelial-specific and expressed in the pancreatic and hepatobiliary ducts.[5] Aberrant *KRT19* expression is crucial in cancer progression. For example, in colon cancer, the knockdown of *KRT19* inhibits tumor progression by downregulating the Wnt/Notch signaling pathway.[6] In breast cancer, *KRT19* silencing blocks the cell cycle and enhances tumor cell apoptosis.[7] Additionally, *KRT19* is highly expressed in thyroid cancer and is correlated with tumor metastasis and staging; *KRT19* knockdown suppresses the proliferation, migration, and epithelial–mesenchymal transition (EMT) of thyroid cancer cell lines.[8] These studies indicated that *KRT19* increases tumor growth by acting as an oncogene. However, the specific function of *KRT19* in PC and the underlying molecular mechanisms remain unknown.

MicroRNAs (miRNAs) are small non-coding RNAs of 19–25 nucleotides in size that control the post-transcriptional silencing of target genes by binding to complementary sequences within the 3′-untranslated region (UTR) of the target mRNA, thereby inducing mRNA degradation or translational repression.[9] Abnormal miRNA expression is involved in several biological processes associated with cancer progression, particularly in PC. For instance, miRNA-217 overexpression in PC inhibits tumor cell aggressiveness and induces apoptosis by activating the AKT pathway by targeting and inhibiting ATAD2, thereby inhibiting PC progression.[10] In solid tumors, excessive tumor growth or compression of blood vessels leads to a hypoxic microenvironment that further promotes tumor progression.[11] Therefore, in this study, we aimed to investigate whether miRNAs control *KRT19* function in PC and further explore the molecular regulatory mechanisms in the hypoxic microenvironment.

[1]The Second Clinical Medical School, Lanzhou University, Lanzhou, China
[2]The First Clinical Medical School, Lanzhou University, Lanzhou, China
[3]Department of General Surgery, The Second Hospital of Lanzhou University, Lanzhou, China
[4]Gansu Province Key Laboratory of Environmental Oncology, The Lanzhou University Second Hospital, Lanzhou, Gansu Province, China
[5]Gansu Province Clinical Nutrition Quality Control Center, The Lanzhou University Second Hospital, Lanzhou, Gansu Province, China
[6]These authors contributed equally
[7]Lead contact
*Correspondence: ery_huizhang@lzu.edu.cn (H.Z.), zhouwc129@163.com (W.-C.Z.)
https://doi.org/10.1016/j.isci.2024.110782

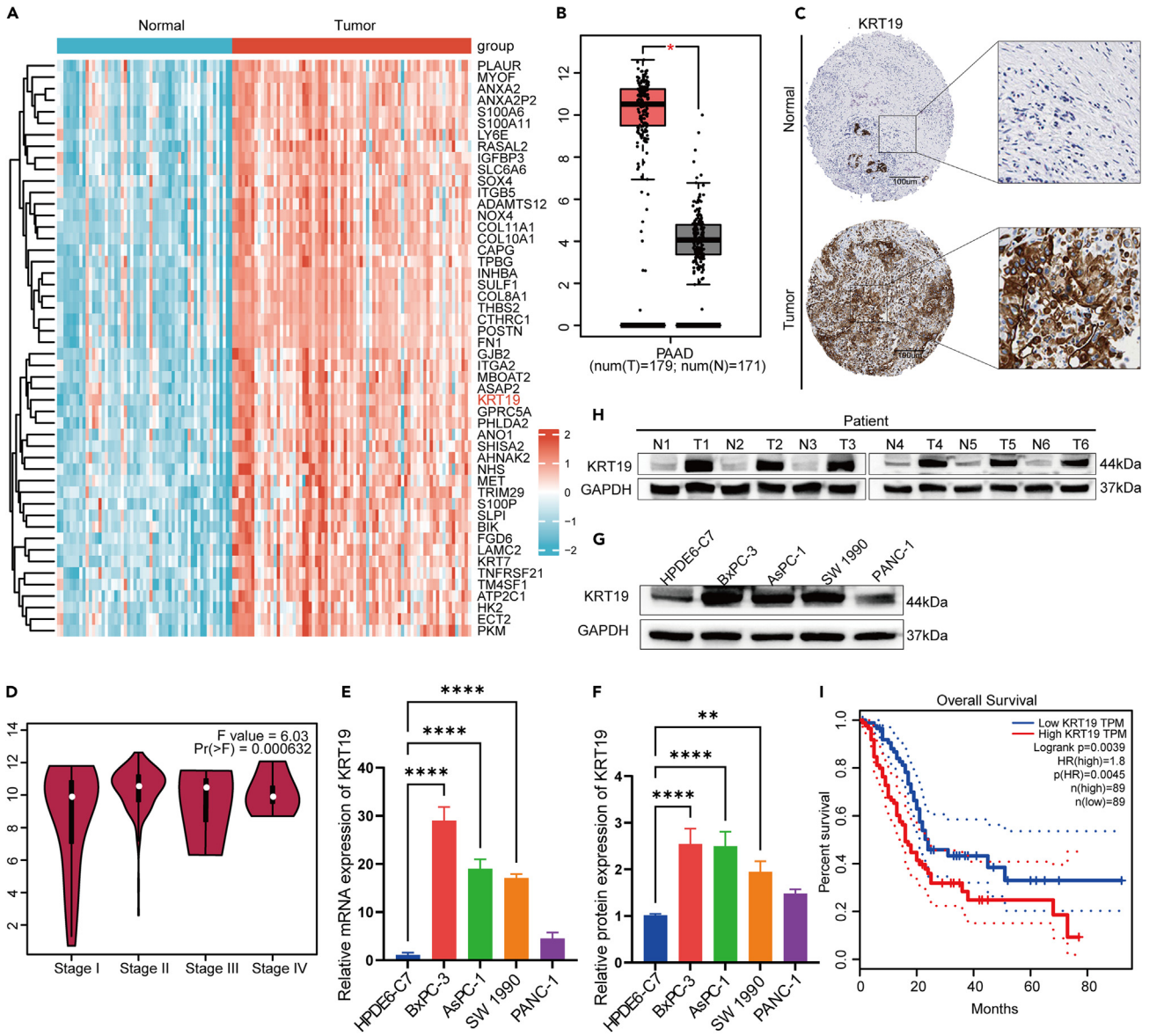

Figure 1. Keratin 19 (*KRT19*) expression is increased in pancreatic cancer (PC) and predicts poor survival

(A) Heatmap visualizing the top 50 differentially expressed genes in GSE15471 and GSE16515, where *KRT19* is upregulated in PC.

(B) GEPIA database outcomes showing significant *KRT19* overexpression in PC tissues compared to healthy tissues.

(C) Immunohistochemical staining revealing significant *KRT19* overexpression in PC tissues from the Human Protein Atlas database. Scale bar = 100 μm.

(D) GEPIA database outcomes representing significant *KRT19* overexpression in different PC stages compared to healthy tissues.

(E) Quantitative reverse transcriptase polymerase chain reaction *KRT19* expression in normal pancreatic epithelial cell lines and PC cell lines (±SD, $n = 3$).

(F and G) Western blot analysis of KRT19 expression in PC cells (±SD, $n = 3$).

(H) Western blotting detected KRT19 expression in 6 pairs of pancreatic cancer and their matched adjacent normal tissues. N: normal adjacent tissue; T: tumor tissue.

(I) Correlation of high *KRT19* expression in GAPIA database with poor prognosis in PC. *$p < 0.05$, **$p < 0.01$, ****$p < 0.0001$.

Herein, *KRT19* showed a high expression in PC and association with worse patient prognosis. Cell and animal experiments showed that *KRT19* promoted the proliferative, migrating, invading, and EMT abilities of PC cells and inhibited apoptosis. The Wnt signaling pathway plays a key role in cancer initiation and progression. In this study, we enriched the Wnt pathway using bioinformatics methods. Subsequent mechanistic investigations confirmed that *KRT19* was negatively regulated by miR-642a-5p, which inhibited PC progression by downregulating *KRT19* and inactivating the Wnt/β-catenin (WBC) pathway.

Table 1. Association between KRT19 expression in tumor and paracancerous tissues and clinicopathological features in 53 pancreatic cancer patients

Variables	n(%)	KRT19 low expression n(%)	KRT19 high expression n(%)	*p*-value
Age	53	13	40	
<60	20 (37.7)	8 (61.5)	12 (30.0)	0.088
≥60	33 (62.3)	5 (38.5)	28 (70.0)	
Gender				
Female	16 (30.2)	3 (23.1)	13 (32.5)	0.768
Male	37 (69.8)	10 (76.9)	27 (67.5)	
Primary site				
Pancreatic head	41 (77.4)	10 (76.9)	31 (77.5)	1
Pancreatic body tail	12 (22.6)	3 (23.1)	9 (22.5)	
AJCC stage				
I,II	46 (86.8)	12 (92.3)	34 (85.0)	0.838
III,IV	7 (13.2)	1 (7.7)	6 (15.0)	
Vascular invasion				
No	36 (67.9)	11 (84.6)	25 (62.5)	0.253
Yes	17 (32.1)	2 (15.4)	15 (37.5)	
Nerve invasion				
No	15 (28.3)	2 (15.4)	13 (32.5)	0.403
Yes	38 (71.7)	11 (84.6)	27 (67.5)	
Lymph node metastasis				
No	29 (54.7)	9 (69.2)	20 (50.0)	0.374
Yes	24 (45.3)	4 (30.8)	20 (50.0)	
Tumor size				
≤2cm	8 (15.1)	1 (7.7)	7 (17.5)	0.008
2-4cm	33 (62.3)	5 (38.5)	28 (70.0)	
>4cm	12 (22.6)	7 (53.8)	5 (12.5)	

RESULTS

KRT19 is overexpressed in PC and predicts a poor prognosis

To identify new PC tumor markers, we analyzed microarray data from the GSE15471 and GSE16515 datasets and observed from DEG expression that *KRT19* was highly expressed in tumor tissues. Combined with a literature review of upregulated candidate genes, we observed that *KRT19* was involved in breast, gastric, and hepatocellular carcinoma (HCC) progression.[12–16] However, its function in PC progression and its exact function and molecular mechanisms have not yet been studied (Figure 1A). Therefore, *KRT19* cells were selected for further experiments. The HPA and GEPIA databases showed that KRT19 was significantly expressed in PC tissues and upregulated with increasing tumor stage (Figures 1B–1D).[17,18] Next, we performed qRT-PCR and western blot analysis on PC cells or tissues and found that KRT19 is highly

Table 2. Spearman correlation analysis between KRT19 expression and clinicopathological characteristics of pancreatic cancer patients

	KRT19 expression	
Variables	Spearman correlation	*p*-value
Age	0.280	0.042
Gender	−0.088	0.529
Primary site	−0.006	0.966
AJCC stage	0.093	0.508
Vascular invasion	0.204	0.143
Nerve invasion	−0.163	0.242
Lymph node metastasis	0.166	0.234
Tumor size	−0.369	0.007

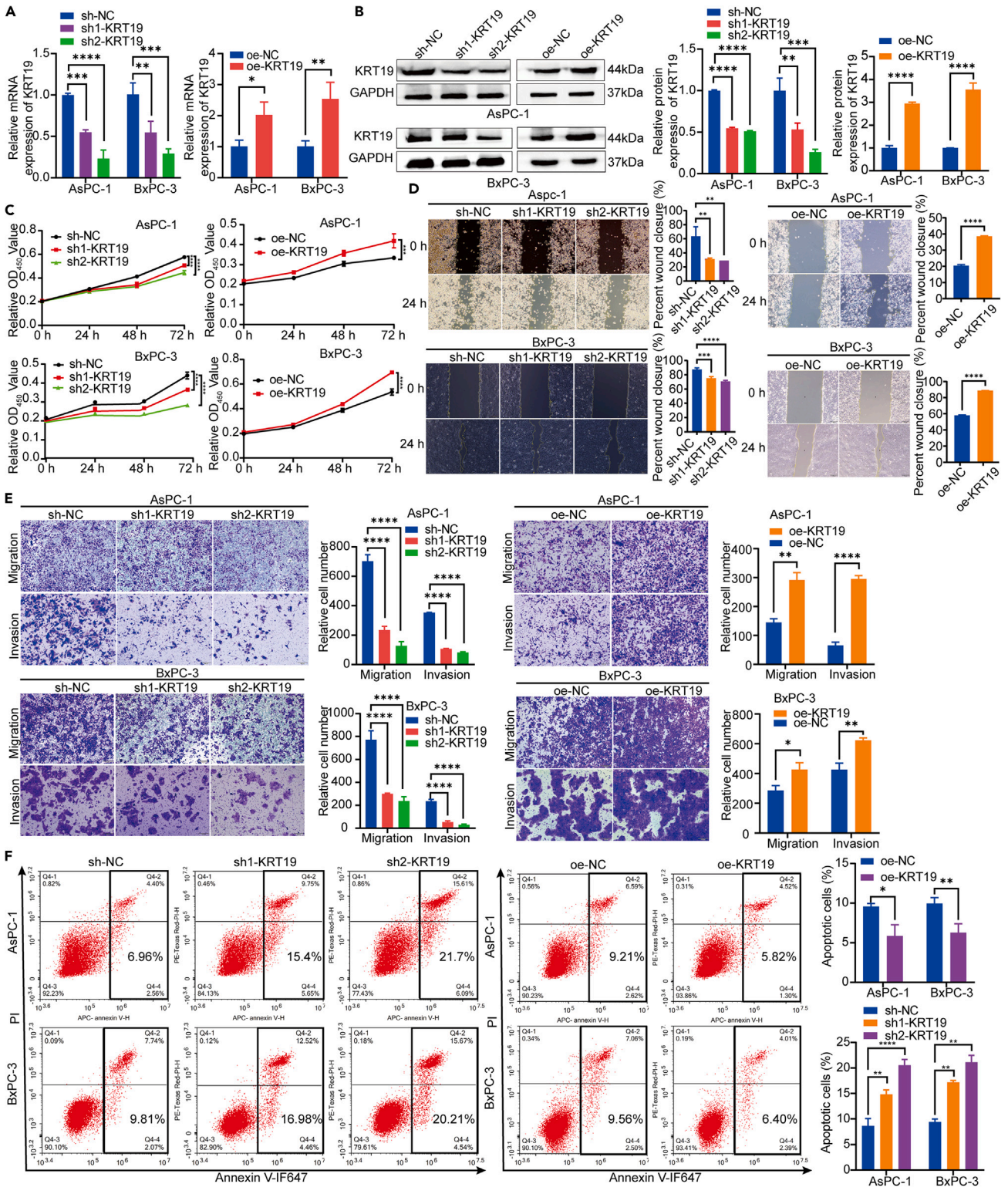

Figure 2. *KRT19* increases pancreatic cancer (PC) cell proliferation and migration with invasion and inhibits apoptosis *in vitro*

(A and B) AsPC-1 and BxPC-3 cells transfected with empty vector (negative control), *KRT19* overexpressing lentivirus (oe-*KRT19*), or *KRT19*-knockdown lentivirus (sh-*KRT19*), detecting the knockdown and overexpression efficiency of *KRT19* through quantitative reverse transcriptase polymerase chain reaction and western blotting (±SD, $n = 3$).

Figure 2. *Continued*

(C) Cell counting Kit-8 assay assessing cell proliferation in the specified cell lines (±SD, $n = 3$).

(D) Wound healing assay assessing the migratory capacity in AsPC-1 and BxPC-3 cells transfected (±SD, $n = 3$). Scale bar = 100 μm.

(E) Transwell assay detects the migration and invasion abilities of these cells (±SD, $n = 3$). Scale bar = 100 μm

(F) Flow cytometry detects apoptosis in these cells (±SD, $n = 3$). *$p < 0.05$, **$p < 0.01$, ***$p < 0.001$, ****$p < 0.0001$.

expressed in PC compared to the normal group. These outcomes were consistent with those of the bioinformatics database study indicated previously (Figures 1E–1H). According to the GEPIA database, patients with PC who had elevated levels of *KRT19* expression possessed significantly lower survival (Figure 1I). We performed PCR on PC tissues and equivalent non-neoplastic tissues from 53 patients to thoroughly determine the correlation between *KRT19* and clinicopathological characteristics. Our analysis revealed a significant correlation between *KRT19* overexpression and tumor size ($p < 0.05$; Table 1). Further analysis using Spearman's correlation demonstrated a significant association between *KRT19* expression and both age and tumor size ($p < 0.05$, Table 2). Collectively, these results suggest that *KRT19* may serve as an adverse prognostic indicator of PC.

KRT19 facilitates PC growth and metastasis *in vitro*

We transfected AsPC-1 and BxPC-3 cell lines with lentiviral vectors, silenced *KRT19* expression using short hairpin RNA, and transfected overexpressing lentiviruses to upregulate *KRT19* expression to understand the role of *KRT19* in PC. Transfection efficiency was assayed at the mRNA and protein concentrations (Figures 2A and 2B). The CCK-8 assay showed that *KRT19* knockdown significantly impeded AsPC-1 and BxPC-3 cell proliferation, whereas *KRT19* overexpression enhanced the growth of both cell lines (Figure 2C). Moreover, WH results showed that the sh-*KRT19* group had a significantly lower scratch width than the control group. However, the oe-KRT19 group reduced the scratch width more significantly (Figure 2D). In addition, transwell assay results revealed that *KRT19* overexpression or knockdown significantly enhanced or impaired AsPC-1 and BxPC-3 cell migration and invasion, respectively (Figure 2E). Flow cytometry techniques were subsequently used to examine cell apoptosis, revealing a significant increase in the number of apoptotic cells in the sh-*KRT19* group as opposed to the control group. Conversely, the overexpression of *KRT19* contributed to a hindrance in apoptosis in AsPC-1 and BxPC-3 cells (Figure 2F). In summary, our results showed that *KRT19* promotes PC cell proliferation, migration, and invasion while simultaneously suppressing apoptosis.

KRT19 knockdown suppresses tumorigenesis *in vivo*

To further demonstrate that *KRT19* promoted PC growth *in vivo*, we created a PC xenograft model in nude mice. Equal numbers of BxPC-3 cells (1×10^6 cells) infected with sh2-KRT19 and sh-NC were subcutaneously injected into the axilla of the forelimbs of male nude mice. The right side represents the control group, and the left side represents the experimental group (Figure 3A). The tumor volume was monitored at intervals of 4 days, and the tumors were removed and weighed on day 28 after injection. The tumor volume in the group in which *KRT19* was silenced was significantly reduced compared to that in the control group (Figure 3B). Moreover, tumors formed in the *KRT19*-knockdown group grew slower and formed smaller tumors than those in the control (Figures 3C and 3D). Sections of the subcutaneous graft tumors were stained. H&E staining revealed less atypia in the nuclei of tumor cells in the sh-*KRT19* group than in the control group, and IHC staining revealed lower expression of KRT19 and Ki67 (Figure 3E). These findings suggest that *KRT19* promotes PC growth *in vivo*, further supporting the tumor-promoting function of *KRT19* in PC.

KRT19 is negatively regulated by miR-642a-5p

To explore the potential mechanisms underlying the role of *KRT19* in PC, we conducted a comprehensive study using three online prediction databases (TargetScan, StarBase, and miRWalk). We discovered three potential upstream regulatory miRNAs (hsa-miR-211-5p, hsa-miR-642a-5p, and hsa-miR-204-5p) (Figure 4A).[19–21] Furthermore, we analyzed these three candidate miRNAs using the StarBase database and observed that miR-642a-5p was downregulated in PC and negatively correlated with *KRT19*; only miR-642a-5p manifested a statistical association with a negative prognosis in PC (Figures 4B–4D). Accordingly, we selected miR-642a-5p for further experiments. We investigated the relationship between miR-642a-5p and *KRT19* using a luciferase reporter assay and demonstrated that miR-642a-5p hindered the luciferase activity of the WT *KRT19* 3′-UTR group, with no variation in the MUT group (Figure 4E). miR-642a-5p mimics or inhibitors were temporarily introduced into AsPC-1 and BxPC-3 cell lines using transfection. Subsequently, we assessed the transfection effectiveness using qRT-PCR (Figure 4F). qRT-PCR and western blotting were used to identify the alterations downstream of *KRT19*. The findings revealed that *KRT19* was overexpressed in PC cells transfected with the miR-642a-5p inhibitor and was downregulated in cells overexpressing miR-642a-5p (Figures 4G and 4H). These results reveal that miR-642a-5p directly targets *KRT19* in PC.

miR-642a-5p suppresses PC cell growth and metastasis

We conducted various functional phenotyping tests to ascertain the role of miR-642a-5p in PC. The CCK-8 assay results demonstrated that the proliferative activity of AsPC-1 and BxPC-3 cells was lower in the group overexpressing miR-642a-5p than in the control group. Conversely, the cell number increased significantly in the group in which miR-642a-5p expression was repressed (Figure 5A). Furthermore, results from the WH and transwell assays showed that elevated miR-642a-5p expression inhibited the ability of PC cells to migrate and invade. Conversely, the group with suppressed miR-642a-5p expression showed significantly enhanced cell migration and invasion (Figures 5B and 5C). Flow

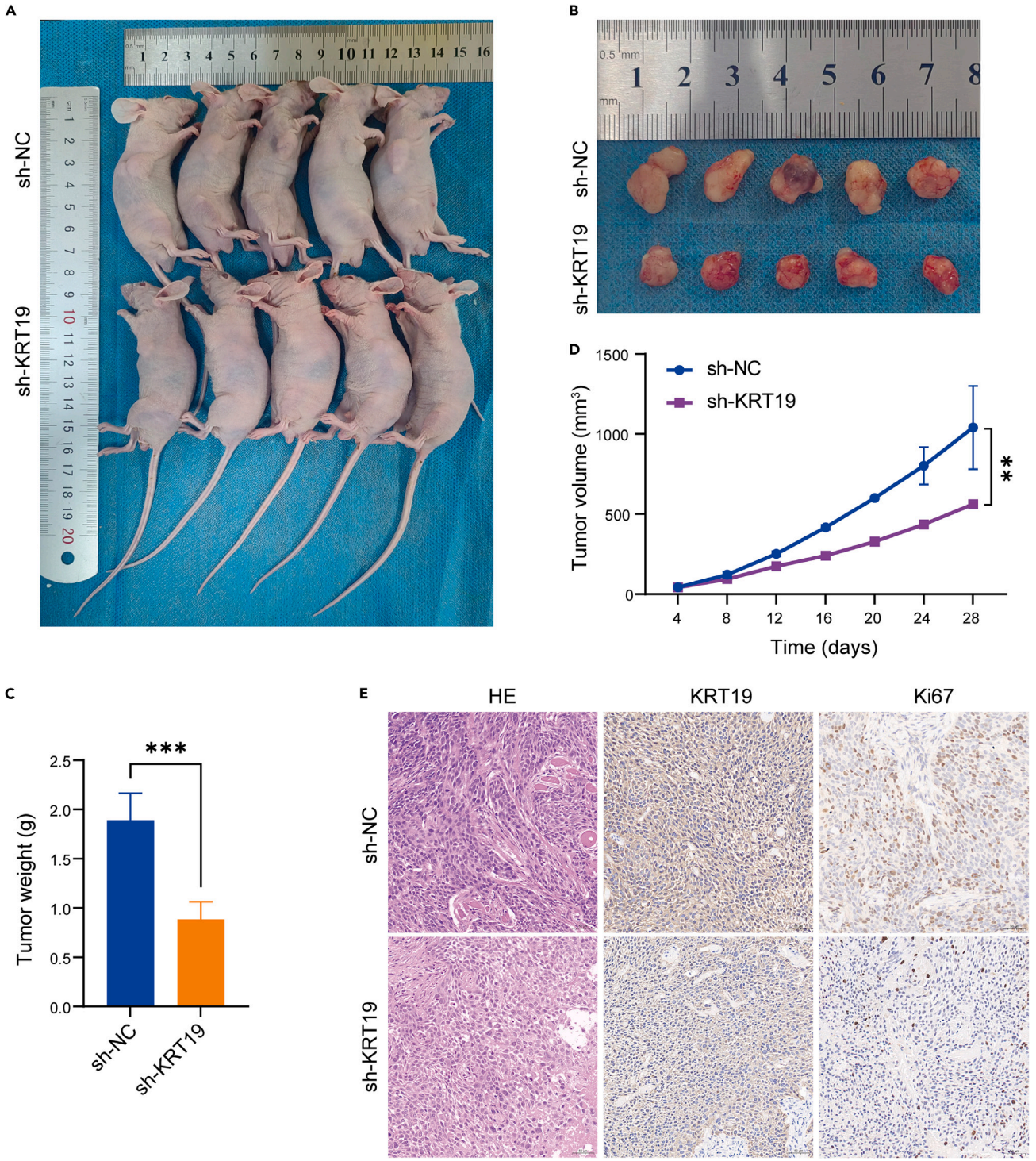

Figure 3. *KRT19* promotes the tumor growth of pancreatic cancer *in vivo*

(A) Subcutaneous tumor nude mouse model image. Hypodermic injection of BxPC-3 cells stably transfected with lentivirus expressing the *KRT19*-knockdown construct (sh-*KRT19*) or control vector (sh-NC) in nude mice.

(B) Subcutaneous xenograft tumor images ($n = 5$ for each group).

(C) Tumor weight of the two groups (±SD, $n = 5$).

(D) Tumor volume measured every 4 days (±SD, $n = 5$).

(E) Representative images showing hematoxylin and eosin stain and KRT19 and Ki-67 immunohistochemistry in xenograft tumors. Scale bar = 50 μm $^{**}p < 0.01$, $^{***}p < 0.001$.

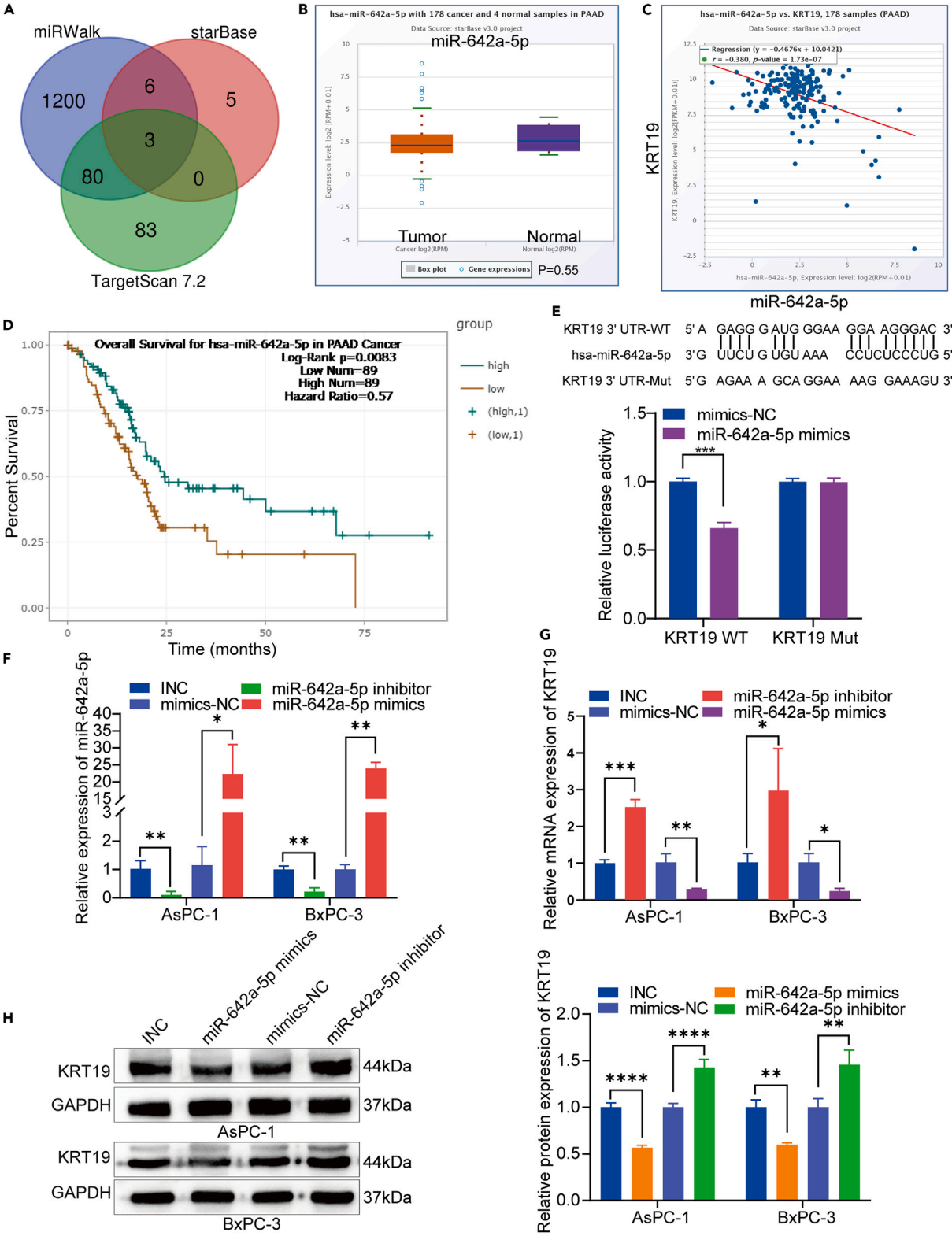

Figure 4. miR-642a-5p directly targets *KRT19* and is correlated with poor prognosis

(A) Venn diagram showing the predicted *KRT19* upstream regulatory miRNAs from three databases (TargetScan, starBase, and miRWalk).

(B) Results from starBase showing miR-642a-5p downregulation in pancreatic cancer (PC) tissues compared to healthy tissues.

Figure 4. *Continued*

(C) miR-642a-5p positive correlation with *KRT19*.

(D) Correlation of miR-642a-5p downregulation with poor prognosis.

(E) Binding site of miR-642a-5p constructed in both the wild-type (WT) 3′-UTR of KRT19 and the matching mutant (Mut) type. The Luciferase reporter assay demonstrated the suppressed luciferase activity of HEK293T cells transfected with the WT 3′-UTR due to miR-642a-5p overexpression (±SD, $n = 5$).

(F) Quantitative reverse transcriptase polymerase chain reaction (qRT-PCR) detection of miR-642a-5p expression after transfection of miR-642a-5p mimics and inhibitors in AsPC-1 and BxPC-3 cells (±SD, $n = 3$).

(G and H) qRT-PCR and western blotting of KRT19 mRNA and protein in cells transfected with miR-642a-5p mimics and inhibitors (±SD, $n = 3$). $^{*}p < 0.05$, $^{**}p < 0.01$, $^{***}p < 0.001$, $^{****}p < 0.0001$.

cytometry results demonstrated that cells transfected with the miR-642a-5p mimic exhibited significantly increased apoptosis. However, the suppression of miR-642a-5p production contributed to decreased apoptosis in PC cells (Figure 5D). Therefore, miR-642a-5p inhibited tumor growth in PC cells by inhibiting cell aggressiveness and stimulating apoptosis.

miR-642a-5p regulates KRT19 functions in PC

We performed rescue experiments by continuing transient transfection of the miR-642a-5p inhibitor in BxPC-3 cells that had originally been stably transfected with *KRT19*-knockdown lentivirus to further ascertain whether *KRT19* affects the inhibitory implications of miR-642a-5p. KRT19 expression was determined through qRT-PCR and western blotting analyses, which showed that KRT19 expression was elevated in the transfected miR-642a-5p inhibitor group and reduced in the sh-*KRT19* group compared to the control. KRT19 expression was partially restored in the co-transfected group (Figures 6A and 6B). The results of the EdU and CCK-8 assays illustrated that silencing miR-642a-5p stimulated PC cell proliferation, and this effect was partially counteracted by *KRT19* knockdown (Figures 6C and 6D). Furthermore, the WH and transwell assay results showed that the ability of PC cells to migrate and invade following the knockdown of miR-642a-5p was significantly reversed by *KRT19* inhibition (Figures 6E and 6F). Subsequently, flow cytometry was used to identify apoptosis, which indicated a more significant number of apoptotic cells in the co-transfected group than in those transfected with the miR-642a-5p inhibitor (Figure 6G). These findings indicate that miR-642a-5p potentially functions as a regulatory factor for *KRT19* and hinders PC growth and advancement by specifically targeting *KRT19*.

KRT19 is regulated by miR-642a-5p and stimulates PC progression through the WBC pathway

We performed GSEA enrichment analysis on DEGs, including *KRT19*, and observed that the WBC pathway was closely correlated with our study (Figure 7A). Moreover, we performed western blotting of the stabilized lentiviral AsPC-1 and BxPC-3 cell lines and observed that KRT19 overexpression elevated the concentrations of β-catenin, c-Myc, cyclin D1, and mesenchymal proteins (N-cadherin and vimentin). *KRT19* knockdown significantly suppressed the expression of WBC- and EMT-related proteins (Figures 7B and 7C). *KRT19* promotes the progression of HCC by stimulating the WBC pathway.[14] Furthermore, expression of mesenchymal-associated proteins in miR-642a-5p inhibitor-transfected BxPC-3 cells were reversed by *KRT19* downregulation (Figure 7D). We observed that Wnt pathway regulation by miR-642a-5p and *KRT19* was blocked by XAV-939 (Figures 7E and 7F). These results suggest that miR-642a-5p negatively regulates *KRT19* expression, suppresses the WBC signaling pathway, and suppresses PC metastasis.

Hypoxia induces miR-642a-5p loss and *KRT19* overexpression in PC

We further investigated the molecular pathways by which the hypoxic microenvironment controls PC progression. First, the analysis from the GEPIA database showed that *KRT19* and HIF1A are positively correlated in PC (Figure 8A). Next, we conducted experiments with PC cells under hypoxic conditions (Figure 8B). To create the hypoxic cell model, we used Western blotting to detect the expression of HIF1α at different time points under hypoxia, and we observed a significant increase in HIF1α expression after 24 h (Figure 8C). The qRT-PCR results indicated that, compared to the normoxic group, HIF1α expression was significantly elevated in AsPC-1 and BxPC-3 cells after hypoxia treatment (Figure 8D). Then, to validate the correlation between *KRT19* and HIF1α, CoIP analysis in the constructed PC hypoxic cell model revealed that HIF1α immunoprecipitates with *KRT19*, whereas no immunoprecipitation occurred under normoxic conditions. Under hypoxia, *KRT19* was overexpressed and co-immunoprecipitated with HIF1α (Figure 8E). qRT-PCR results showed that *KRT19* expression was significantly increased in cells after 24 h of hypoxia compared to the normoxic group, while the expression of the upstream miR-642a-5p was downregulated (Figures 8F and 8G). Finally, further validation showed that knocking down HIF1α expression in PC cells under hypoxic conditions led to an increase in miR-642a-5p expression (Figures 8H and 8I). Collectively, these results suggest that hypoxia-induced miR-642a-5p loss and *KRT19* overexpression may lead to the malignant phenotype of PC.

DISCUSSION

PC is an aggressive tumor that poses a considerable danger to human health.[22] This type of cancer usually does not show early symptoms and is often detected at an advanced stage, when the 5-year survival rate is typically below 10%.[23] Early surgical removal and chemotherapy can somewhat hinder PC progression; however, most patients survive for only a few months to a year because of early postoperative relapse and resistance to chemotherapeutic drugs.[24] The emergence of new treatment methods and technologies, such as immunotherapy and precision medicine, is promising for patients with PC; however, these techniques remain in the research phase.[25] Therefore, identifying effective targets

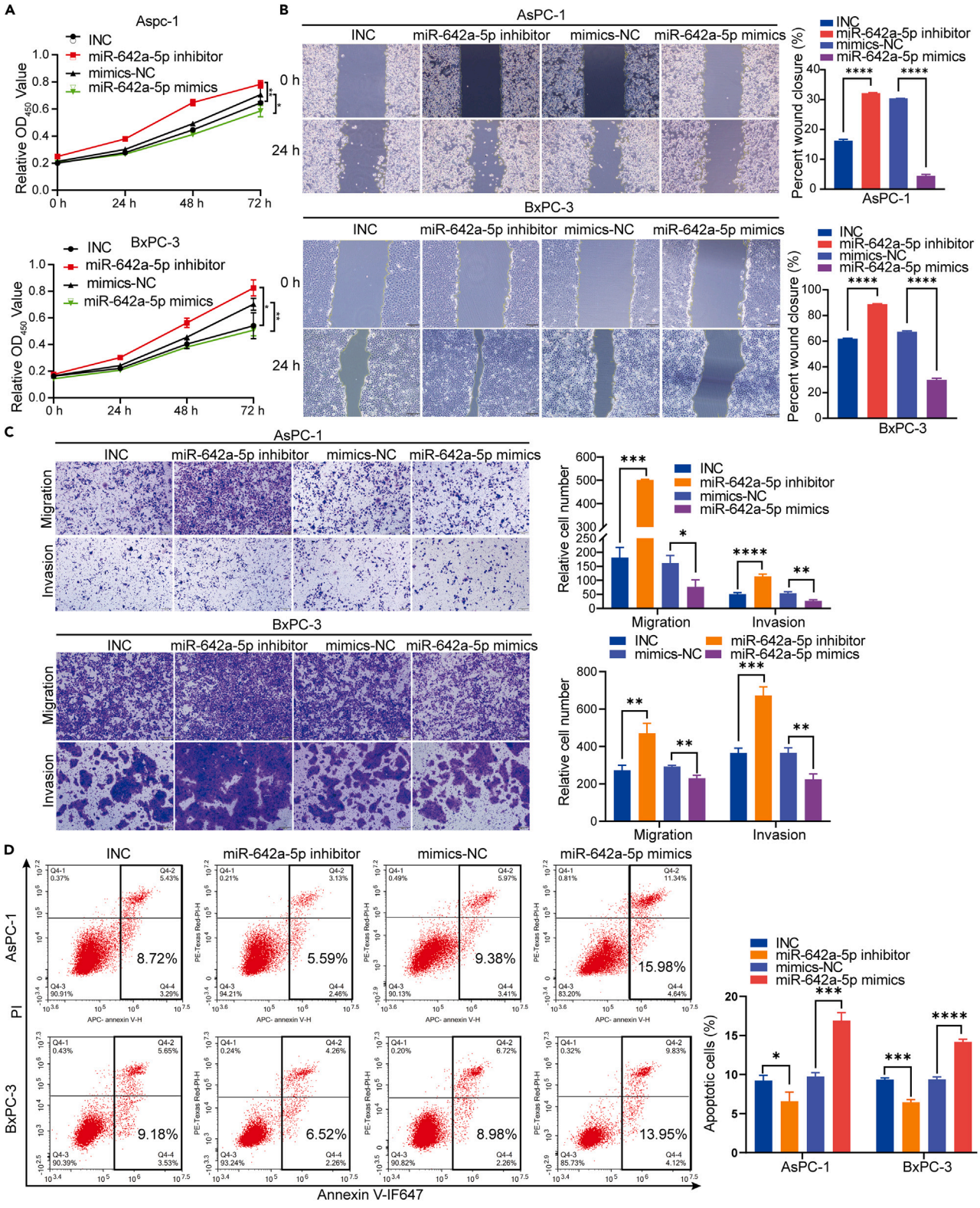
A
Aspc-1
INC
miR-642a-5p inhibitor
mimics-NC
miR-642a-5p mimics
Relative OD450 Value
0 h
24 h
48 h
72 h
BxPC-3
B
AsPC-1
INC
miR-642a-5p inhibitor
mimics-NC
miR-642a-5p mimics
0 h
24 h
Percent wound closure (%)
BxPC-3
C
AsPC-1
Migration
Invasion
Relative cell number
BxPC-3
D
AsPC-1
BxPC-3
PI
Annexin V-IF647
APC- annexin V-H
PE-Texas Red-PI-H
8.72%
5.59%
9.38%
15.98%
9.18%
6.52%
8.98%
13.95%
Apoptotic cells (%)

Figure 5. miR-642a-5p suppresses pancreatic cancer (PC) cell proliferation, migration, and invasion and increases apoptosis

(A) CCK-8 assay detects cell proliferative capacity in AsPC-1 and BxPC-3 cells transfected with miR-642a-5p mimics or inhibitors (±SD, $n = 3$).

(B) Migratory ability of PC cells after miR-642a-5p knockdown or overexpression was determined by wound healing (WH) assay. WH images at 0 and 24 h following scratching (±SD, $n = 3$). Scale bar = 100 μm.

(C) Transwell assays detecting cell migration and invasion in PC cells transfected with miR-642a-5p mimics or inhibitors (±SD, $n = 3$). Scale bar = 100 μm.

(D) Flow cytometry assessing apoptosis (±SD, $n = 3$). *$p < 0.05$, **$p < 0.01$, ***$p < 0.001$, ****$p < 0.0001$.

for PC treatment is important. In this study, we elaborated on the role and regulatory mechanism of *KRT19* in PC and observed that inhibiting *KRT19* can suppress PC development.

KRT19 expression is involved in the biological processes and prognosis of several types of malignancies. In lung cancer, elevated *KRT19* expression is associated with shorter prognostic overall survival and is considered a potential molecular marker.[26] In HCC, *KRT19* is significantly upregulated and positively associated with greater tumor size, more severe microvascular infiltration, more intrahepatic metastases, and lower survival.[14] In breast cancer, the knockdown of *KRT19* inhibits the proliferative activity of tumor cells and is considered a potential biomarker.[27] In the present study, *KRT19* was significantly upregulated in PC tissues and cells, and its elevated expression correlated with some clinicopathological features such as patient age and tumor size. However, *KRT19* expression did not show a significant difference in tumor staging compared to the analysis of datasets from the GEPIA database, which might be attributed to the limited number of clinical samples collected ($n = 53$). *KRT19* knockdown significantly suppressed PC cell proliferation, migration, invasion, and EMT while promoting apoptosis. In a subcutaneous tumor experiment in nude mice, the tumor volume in the sh-*KRT19* group was significantly lower than that in the control group. However, *KRT19* overexpression significantly enhanced PC cell growth and migration. These results suggested that *KRT19* facilitates tumor growth and metastasis in PC.

The WBC pathway is frequently overactive in tumor tissues and is significantly associated with malignant advancement and poor tumor prognosis.[28] β-catenin is crucial as a pivotal protein in the Wnt signaling pathway. β-catenin migrates to the nucleus and activates the transcription of the downstream target genes, c-Myc, and cyclin D1, promoting the malignant progression of cells upon stimulation of the signaling pathway.[29] In colon cancer, an interaction was observed between *KRT19* and β-catenin, which facilitates the proliferation and migration of tumor cells.[6] Another study showed that a WBC pathway inhibitor (XAV-939) significantly reversed the tumor-promoting effect on PC cells.[30] In the present study, western blotting results showed a significant hindrance in β-catenin, c-Myc, and cyclin D1 and promoted the expression of E-cadherin in PC cells transfected with sh-*KRT19*. Conversely, in overexpressing cells, a significant increase was observed in the expression of the WBC pathway-related proteins N-cadherin and vimentin. For further validation, we added XAV-939 to cells overexpressing *KRT19* and discovered that the promoting effects of *KRT19* on β-catenin were reversed. These results suggest that *KRT19* increases the growth and EMT of PC cells by stimulating the WBC signaling pathway.

miRNAs are indispensable in the development and progression of tumors.[31] In the present study, we first detected that miR-642a-5p may target and regulate *KRT19* in PC through bioinformatics analysis. Subsequent dual-luciferase reporter gene experiments validated this finding, demonstrating that *KRT19* is an miR-642a-5p target gene. Previous studies have suggested that miR-642a-5p expression is significantly reduced in prostate cancer and has a poor prognosis. The results of *in vivo* and *in vitro* experiments demonstrated that miR-642a-5p overexpression significantly suppressed tumor growth, indicating its role in suppressing prostate cancer.[32] In colorectal cancer, the upregulation of miR-642a-5p significantly inhibits the vitality, migration, invasion, and EMT of tumor cells.[33] In the present study, we transfected miR-642a-5p mimics into AsPC-1 and BxPC-3 cells, revealing that downstream *KRT19* expression decreased. miR-642a-5p upregulation inhibited the growth and migration of PC cells and promoted apoptosis. Conversely, miR-642a-5p knockdown increased *KRT19* expression as well as tumor cell proliferation, migration, invasion, and EMT. Additionally, the results of the restoration experiment showed that the promoting effects of downregulating miR-642a-5p in PC cells were partially reversed by knocking down *KRT19*. Furthermore, we introduced XAV-939 into PC cells transfected with miR-642a-5p and observed a reversal in the stimulatory effect of miR-642a-5p on β-catenin. These findings indicated that in PC, miR-642a-5p directly targets and suppresses the activity of *KRT19*, preventing its tumor-suppressive function by regulating the WBC pathway.

The hypoxic microenvironment is a prominent feature of solid tumors and has received increasing research interest for developing pre-tumor treatments, which is significantly correlated with poor prognosis in different tumors, including PC and gastric, breast, and liver cancers.[34–37] A hypoxic environment can lead to the production of more metabolic products and acidic substances by tumor cells, increasing the acidity of the tumor tissue, and thereby affecting drug penetration and treatment effectiveness.[38] During hypoxia, upregulation of HIF1α expression promotes EMT and metastatic phenotypes.[39] A hypoxic environment is also a key factor in PC metastasis, leading to abnormal expression of miRNAs and related genes.[40–42] Therefore, we attempted to determine the role of hypoxia on miR-642a-5p and *KRT19* expression in PC. In our study, we observed that HIF1α expression was elevated during hypoxia in AsPC-1 and BxPC-3 cells. Compared to that in the normoxic group, miR-642a-5p was expressed at lower levels under hypoxic conditions while promoting the expression of *KRT19*. The results of CoIP experiments verified the interaction between HIF1α and *KRT19*. Further research revealed that knocking down HIF1α increased miR-642a-5p expression. These results indicated that hypoxia induced the loss of miR-642a-5p and overexpression of *KRT19*.

Overall, we observed that KRT19 was significantly expressed in both PC tissues and cell lines. Furthermore, this increased expression is closely related to malignant clinical–pathological characteristics. Additionally, we showed that miR-642a-5p exerted a negative regulatory effect on *KRT19*. This miRNA inhibited PC cell proliferation, migration, invasion, and EMT by directly targeting the WBC pathway, which is mediated by *KRT19* while promoting cell death. Hypoxia is crucial in the inadequate expression of miR-642a-5p and elevated *KRT19* expression in PC cells. Therefore, *KRT19* facilitates the advancement of PC and may be a new prognostic indicator and a possible target for therapeutic interventions.

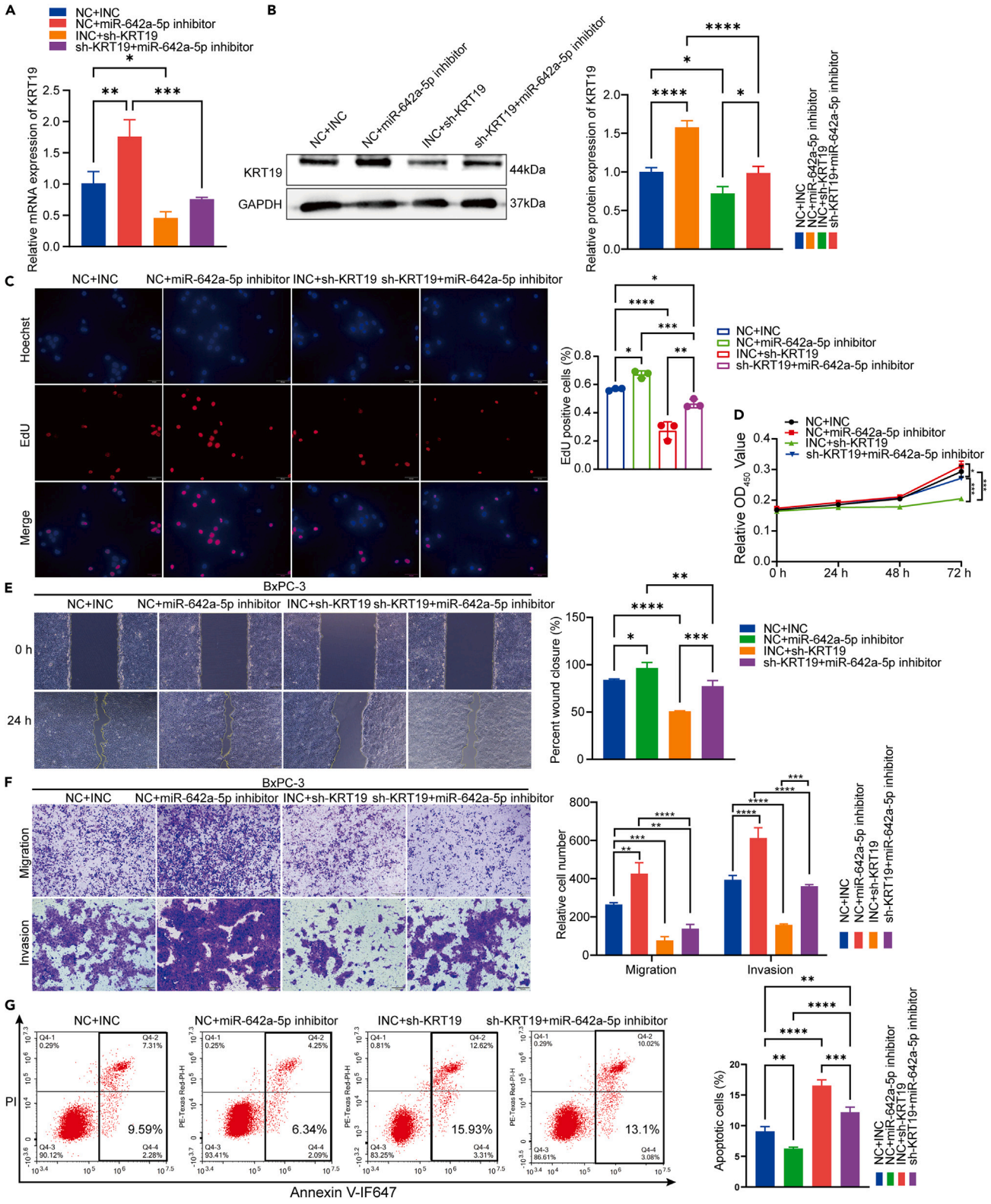

Figure 6. *KRT19* roles in pancreatic cancer (PC) are regulated by miR-642a-5p

BxPC-3 cells transfected with sh-NC integrated inhibitor-NC, sh-NC combined miR-642a-5p inhibitor, sh-*KRT19* integrated inhibitor-NC, or sh-*KRT19* combined miR-642a-5p inhibitor.

Figure 6. *Continued*

(A and B) *KRT19* expression measured via quantitative reverse transcriptase polymerase chain reaction and western blotting (±SD, $n = 3$).

(C and D) *KRT19* knockdown effectively alleviates the suppression of miR-642a-5p inhibitor on the proliferative activity of BxPC-3 cells, as evidenced by EdU and CCK-8 experiments (±SD, $n = 3$). Scale bar = 50 μm.

(E) *KRT19* downregulation partially reverses the suppressive effect of miR-642a-5p on PC cell migration, as indicated by the wound healing assay (±SD, $n = 3$). Scale bar = 100 μm.

(F) *KRT19* downregulation partially reversed the suppressive effect of miR-642a-5p on PC cell migration and invasion ability, as evidenced by the transwell assay (±SD, $n = 3$). Scale bar = 100 μm. (G) Flow cytometry detects cell apoptosis (±SD, $n = 3$). *$p < 0.05$, **$p < 0.01$, ***$p < 0.001$, ****$p < 0.0001$.

Conclusions

We discovered that *KRT19* levels were higher in PC tissues, which was significantly associated with a poor prognosis in patients with PC. *KRT19* suppression hampers tumor growth, spread, and formation in PC cells *in vivo*. Moreover, miR-642a-5p functions as a tumor suppressor by exerting a negative regulatory effect on *KRT19* expression. Hypoxia-induced miR-642a-5p deficiency and *KRT19* overexpression create a favorable environment for tumor growth and promote PC progression. The mechanism by which miR-642a-5p inhibits PC progression may involve targeting the WBC pathway mediated by *KRT19*, which plays a crucial role in this process. This finding provides a deeper understanding of the mechanisms underlying cancer progression and new targets for the molecular therapy of PC.

Limitations of the study

First, in the animal experiments section, this study did not build a distant metastasis model, and it did not explore the impact of KRT19 inhibitors on PC treatment. Second, in the pathway research, the effect of pathway changes on the phenotype was not verified. Lastly, there was no research conducted on the relationship between hypoxic microenvironments and tumor immunity. All these factors need further investigation in future experiments.

RESOURCE AVAILABILITY

Lead contact

Further information and requests for resources and reagents should be directed to and will be fulfilled by the lead contact, W.-C.Z. (zhouwc129@163.com).

Materials availability

This study did not generate new unique reagents and all materials in this study are commercially available.

Data and code availability

- RNA-sequencing data was deposited at GEO and are publicly available as of the date of publication. Accession numbers are listed in the key resources table.
- This article does not report original code.
- Any additional information required to reanalyze the data reported in this paper is available from the lead contact upon request.

ACKNOWLEDGMENTS

We would like to thank Editage (www.editage.cn) for the English language editing. This study was supported by the National Natural Science Foundation of China (82260555), Medical Innovation and Development Project of Lanzhou University (lzuyxcx-2022-177), Science and Technology Projects of Chengguan District in Lanzhou (2023-11-2), Joint Research Fund General Projects of Gansu Province (23JRRA1508), Gansu Youth Science and Technology Fund (24JRRA374), The Second Hospital of Lanzhou University "Cuiying Science and Technology Innovation" Program (CY2023-YB-A02), and Major Science and Technology Projects of Gansu Province (22ZD6FA021-4).

AUTHOR CONTRIBUTIONS

H.-Q.S., H.Z., and W.-C.Z. contributed to the conceptualization and design of the study. H.-Q.S. and X.L. conducted experiments and wrote the manuscript. H.-Q.S., X.L., Z.C., and S.D. conducted functional experiments. H.-Q.S., X.L., C.Y., and S.H. assisted with the animal experiments. H.-Q.S. and X.L. analyzed the data. H.-Q.S., Z.C., and D.-A.F. collected experimental data. W.-C.Z. and H.Z. revised the manuscript and supervised the experimental procedures, with H.Z. as co-corresponding author. X.L. contributed equally to this work and should be considered the first co-author. All the authors have read and approved the final version of the manuscript.

DECLARATION OF INTERESTS

The authors declare no competing financial interests.

STAR★METHODS

Detailed methods are provided in the online version of this paper and include the following:

- KEY RESOURCES TABLE
- EXPERIMENTAL MODEL AND STUDY PARTICIPANT DETAILS
  - Patients with PC
  - Cell culture

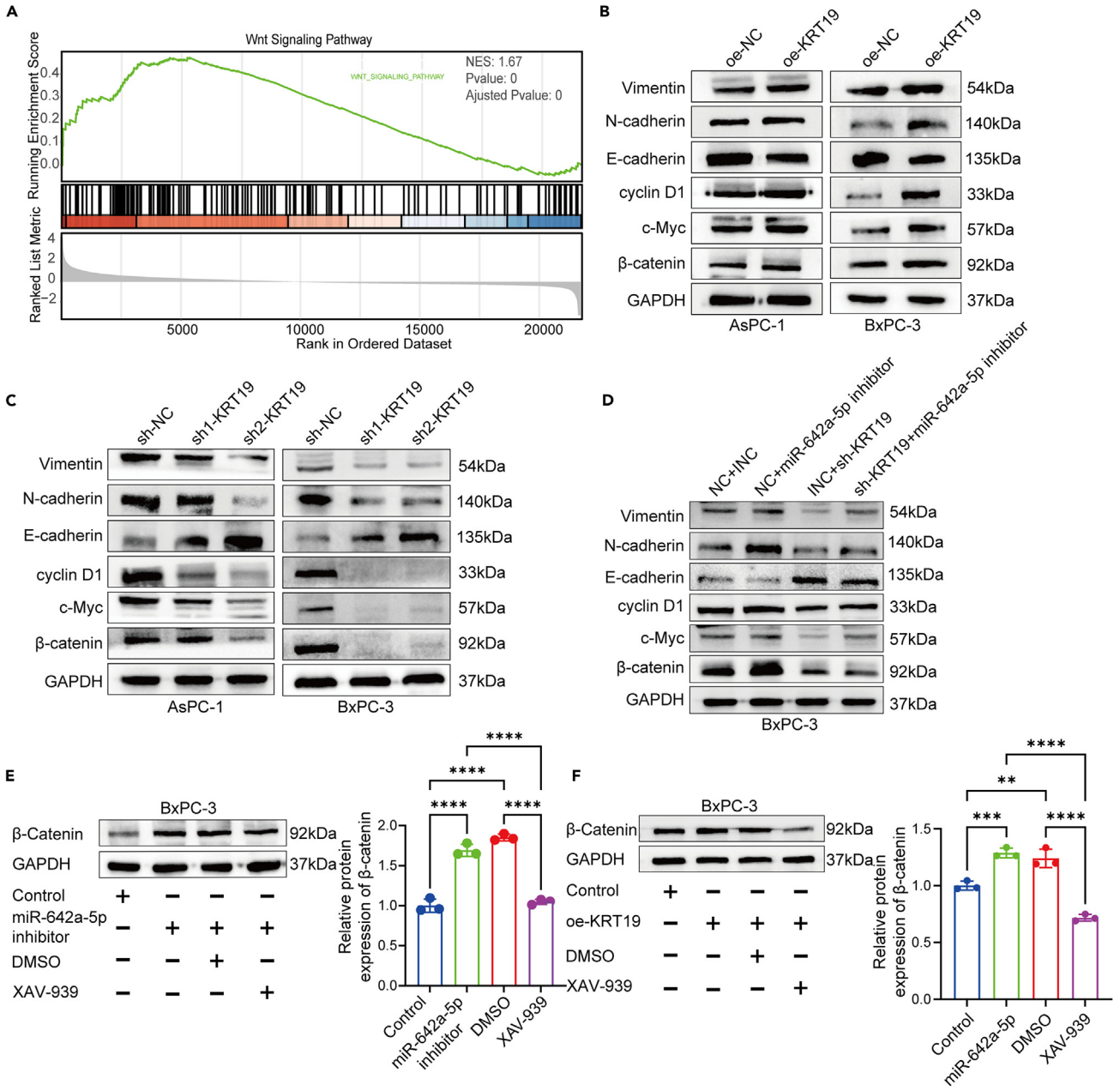

Figure 7. *KRT19* is regulated by miR-642a-5p and promotes pancreatic cancer (PC) progression through the Wnt/β-catenin (WBC) pathway

(A) Wnt signaling pathway was identified in differentially expressed genes through gene set enrichment analysis.

(B and C) Western blotting (WB) analysis of the implications of KRT19 overexpression or knockdown on the WBC pathway and epithelial–mesenchymal transition (EMT)-related proteins.

(D) KRT19 inhibition in BxPC-3-*anti*-miR-642a-5p cells partially counteracts the suppressive impact of miR-642a-5p on the WBC pathway and EMT-related proteins, as indicated by WB analysis.

(E and F) BxPC-3 cells with miR-642a-5p knockdown or overexpressed *KRT19* treated with the WBC signaling pathway inhibitor XAV-939 (10 μmol/L) for 24 h, assessing the protein expression using WB (±SD, $n = 3$). $^{**}p < 0.01$, $^{***}p < 0.001$, $^{****}p < 0.0001$.

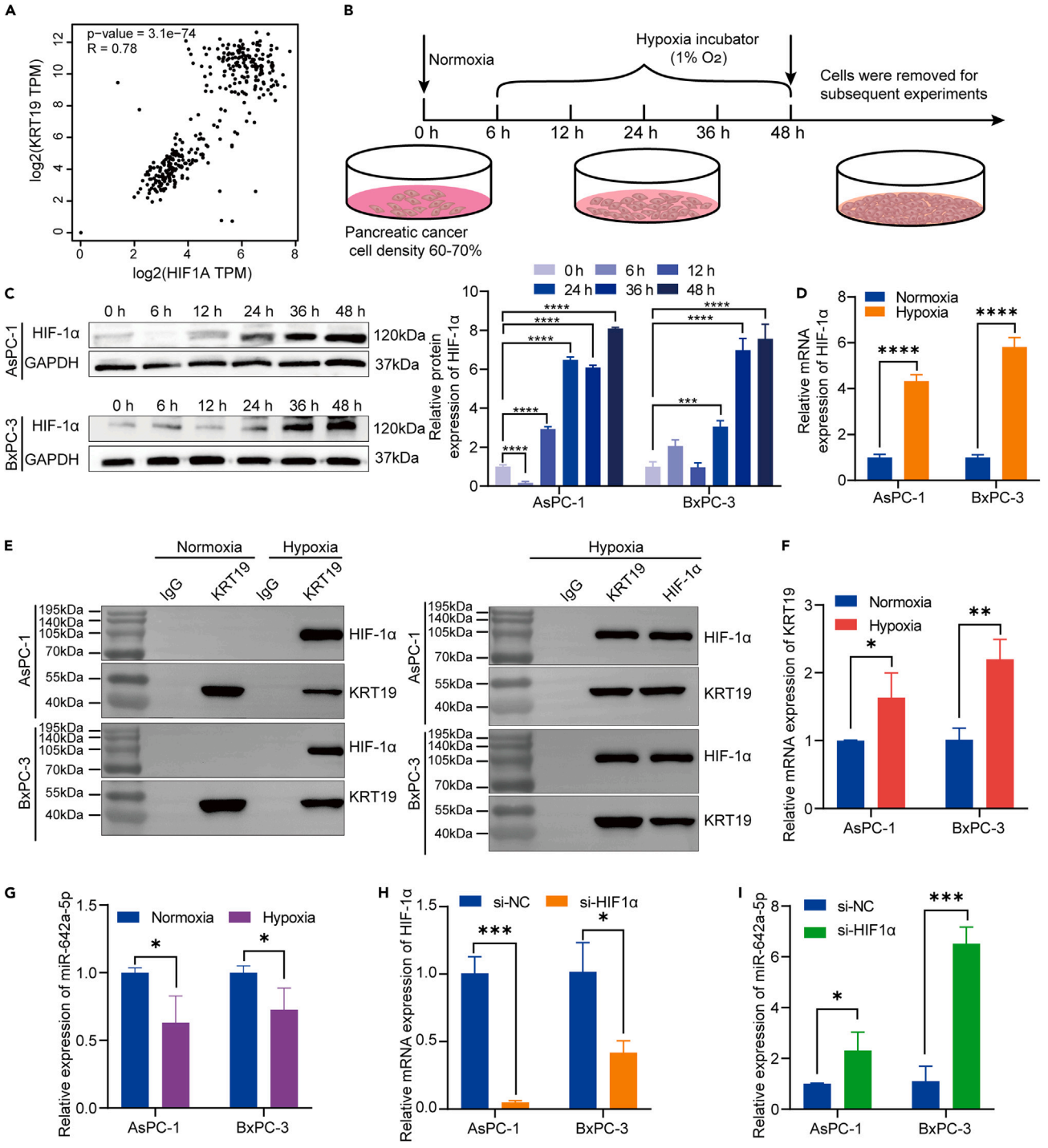

Figure 8. Hypoxia induces miR-642a-5p loss and *KRT19* upregulation in pancreatic cancer (PC) cells

(A) GEPIA database analysis showing a positive *KRT19* correlation with *HIF1A* in PC.

(B) Flow chart of hypoxic modeling at different time intervals.

(C) Western blotting detection and quantification of HIF1α expression in AsPC-1 and BxPC-3 cells under hypoxic or normoxic conditions (±SD, $n = 3$).

(D) Determining HIF1α expression under both hypoxic and normoxic conditions employing quantitative reverse transcriptase polymerase chain reaction (±SD, $n = 3$).

(E) Co-immunoprecipitation analysis of the HIF1α-KRT19 interaction in cells treated as specified.

Figure 8. *Continued*

(F and G) qRT-PCR analysis of KRT19 and miR-642a-5p expression in AsPC-1 and BxPC-3 cells under hypoxia and normoxia (±SD, $n = 3$).

(H) Relative expression of HIF1α in AsPC-1 and BxPC-3 cells transfected with short hairpin RNA targeting HIF1α (si-HIF1α), ascertained through qRT-PCR (±SD, $n = 3$). (I) miR-642a-5p relative expression following transfection with si-HIF1α under hypoxic conditions (±SD, $n = 3$). *$p < 0.05$, **$p < 0.01$, ***$p < 0.001$, ****$p < 0.0001$.

- Wound healing (WH) assay
- Transwell assays
- Flow cytometry
- Luciferase reporter assay
- Immunohistochemistry
- 5-Ethynyl-2′-deoxyuridine (EdU) experiment
- Co-immunoprecipitation (CoIP) assay
- Bioinformatics analysis

- QUANTIFICATION AND STATISTICAL ANALYSIS

SUPPLEMENTAL INFORMATION

Supplemental information can be found online at https://doi.org/10.1016/j.isci.2024.110782.

Received: May 9, 2024
Revised: June 19, 2024
Accepted: August 18, 2024
Published: August 22, 2024

REFERENCES

1. Sung, H., Ferlay, J., Siegel, R.L., Laversanne, M., Soerjomataram, I., Jemal, A., and Bray, F. (2021). Global Cancer Statistics 2020: GLOBOCAN Estimates of Incidence and Mortality Worldwide for 36 Cancers in 185 Countries. CA A Cancer J. Clin. *71*, 209–249. https://doi.org/10.3322/caac.21660.
2. Urbanova, M., Cihova, M., Buocikova, V., Slopovsky, J., Dubovan, P., Pindak, D., Tomas, M., García-Bermejo, L., Rodríguez-Garrote, M., Earl, J., et al. (2023). Nanomedicine and epigenetics: New alliances to increase the odds in pancreatic cancer survival. Biomed. Pharmacother. *165*, 115179. https://doi.org/10.1016/j.biopha.2023.115179.
3. Cai, J., Chen, H., Lu, M., Zhang, Y., Lu, B., You, L., Zhang, T., Dai, M., and Zhao, Y. (2021). Advances in the epidemiology of pancreatic cancer: Trends, risk factors, screening, and prognosis. Cancer Lett. *520*, 1–11. https://doi.org/10.1016/j.canlet.2021.06.027.
4. Berens, E.B., Sharif, G.M., Schmidt, M.O., Yan, G., Shuptrine, C.W., Weiner, L.M., Glasgow, E., Riegel, A.T., and Wellstein, A. (2017). Keratin-associated protein 5-5 controls cytoskeletal function and cancer cell vascular invasion. Oncogene *36*, 593–605. https://doi.org/10.1038/onc.2016.234.
5. Brembeck, F.H., Moffett, J., Wang, T.C., and Rustgi, A.K. (2001). The keratin 19 promoter is potent for cell-specific targeting of genes in transgenic mice. Gastroenterology *120*, 1720–1728.
6. Saha, S.K., Yin, Y., Chae, H.S., and Cho, S.-G. (2019). Opposing Regulation of Cancer Properties via KRT19-Mediated Differential Modulation of Wnt/β-Catenin/Notch Signaling in Breast and Colon Cancers. Cancers *11*, 99. https://doi.org/10.3390/cancers11010099.
7. Sharma, P., Alsharif, S., Bursch, K., Parvathaneni, S., Anastasakis, D.G., Chahine, J., Fallatah, A., Nicolas, K., Sharma, S., Hafner, M., et al. (2019). Keratin 19 regulates cell cycle pathway and sensitivity of breast cancer cells to CDK inhibitors. Sci. Rep. *9*, 14650. https://doi.org/10.1038/s41598-019-51195-9.
8. Wang, X., Xu, X., Peng, C., Qin, Y., Gao, T., Jing, J., and Zhao, H. (2019). BRAFV600E-induced KRT19 expression in thyroid cancer promotes lymph node metastasis via EMT. Oncol. Lett. *18*, 927–935. https://doi.org/10.3892/ol.2019.10360.
9. Lu, T.X., and Rothenberg, M.E. (2018). MicroRNA. J. Allergy Clin. Immunol. *141*, 1202–1207. https://doi.org/10.1016/j.jaci.2017.08.034.
10. Dutta, M., Das, B., Mohapatra, D., Behera, P., Senapati, S., and Roychowdhury, A. (2022). MicroRNA-217 modulates pancreatic cancer progression via targeting ATAD2. Life Sci. *301*, 120592. https://doi.org/10.1016/j.lfs.2022.120592.
11. Chen, Z., Han, F., Du, Y., Shi, H., and Zhou, W. (2023). Hypoxic microenvironment in cancer: molecular mechanisms and therapeutic interventions. Signal Transduct. Targeted Ther. *8*, 70. https://doi.org/10.1038/s41392-023-01332-8.
12. Mi, L., Liang, N., and Sun, H. (2022). A Comprehensive Analysis of KRT19 Combined with Immune Infiltration to Predict Breast Cancer Prognosis. Genes *13*, 1838. https://doi.org/10.3390/genes13101838.
13. Yang, Z., Yan, C., Liu, W., Xu, W., Li, C., Yan, M., Liu, B., and Zhu, Z. (2021). Identification of novel autoantibodies in ascites of relapsed paclitaxel-resistant gastric cancer with peritoneal metastasis using immunome protein microarrays and proteomics. Cancer Biomarkers *31*, 329–338. https://doi.org/10.3233/CBM-203142.
14. Zhang, X., Xu, X., Zhang, Z., Xue, C., Kong, Z., Wu, S., Yun, X., Fu, Y., Zhu, C., and Qin, X. (2021). Linc-KILH potentiates Notch1 signaling through inhibiting KRT19 phosphorylation and promotes the malignancy of hepatocellular carcinoma. Int. J. Biol. Sci. *17*, 768–780. https://doi.org/10.7150/ijbs.52279.
15. Pei, H., Li, L., Fridley, B.L., Jenkins, G.D., Kalari, K.R., Lingle, W., Petersen, G., Lou, Z., and Wang, L. (2009). FKBP51 affects cancer cell response to chemotherapy by negatively regulating Akt. Cancer Cell *16*, 259–266. https://doi.org/10.1016/j.ccr.2009.07.016.
16. Barrett, T., Wilhite, S.E., Ledoux, P., Evangelista, C., Kim, I.F., Tomashevsky, M., Marshall, K.A., Phillippy, K.H., Sherman, P.M., Holko, M., et al. (2013). NCBI GEO: archive for functional genomics data sets–update. Nucleic Acids Res. *41*, D991–D995. https://doi.org/10.1093/nar/gks1193.
17. Tang, Z., Li, C., Kang, B., Gao, G., Li, C., and Zhang, Z. (2017). GEPIA: a web server for cancer and normal gene expression profiling and interactive analyses. Nucleic Acids Res. *45*, W98–W102. https://doi.org/10.1093/nar/gkx247.
18. Uhlén, M., Fagerberg, L., Hallström, B.M., Lindskog, C., Oksvold, P., Mardinoglu, A., Sivertsson, Å., Kampf, C., Sjöstedt, E., Asplund, A., et al. (2015). Proteomics. Tissue-based map of the human proteome. Science (New York, N.Y.) *347*, 1260419. https://doi.org/10.1126/science.1260419.
19. Riffo-Campos, Á.L., Riquelme, I., and Brebi-Mieville, P. (2016). Tools for Sequence-Based miRNA Target Prediction: What to Choose? Int. J. Mol. Sci. *17*, 1987.
20. Dweep, H., and Gretz, N. (2015). miRWalk2.0: a comprehensive atlas of microRNA-target interactions. Nat. Methods *12*, 697. https://doi.org/10.1038/nmeth.3485.
21. Li, J.-H., Liu, S., Zhou, H., Qu, L.-H., and Yang, J.-H. (2014). starBase v2.0: decoding miRNA-ceRNA, miRNA-ncRNA and protein-RNA interaction networks from large-scale CLIP-Seq data. Nucleic Acids Res. *42*, D92–D97. https://doi.org/10.1093/nar/gkt1248.
22. Advancing on pancreatic cancer (2021). Nature Reviews. Gastroenterol. Hepatol. *18*, 447. https://doi.org/10.1038/s41575-021-00479-5.
23. Siegel, R.L., Miller, K.D., Wagle, N.S., and Jemal, A. (2023). Cancer statistics, 2023. CA A

Cancer J. Clin. *73*, 17–48. https://doi.org/10.3322/caac.21763.

24. Zhao, Y., Qin, C., Zhao, B., Wang, Y., Li, Z., Li, T., Yang, X., and Wang, W. (2023). Pancreatic cancer stemness: dynamic status in malignant progression. J. Exp. Clin. Cancer Res. *42*, 122. https://doi.org/10.1186/s13046-023-02693-2.
25. Bose, M., Sanders, A., De, C., Zhou, R., Lala, P., Shwartz, S., Mitra, B., Brouwer, C., and Mukherjee, P. (2023). Targeting tumor-associated MUC1 overcomes anoikis-resistance in pancreatic cancer. Transl. Res. *253*, 41–56. https://doi.org/10.1016/j.trsl.2022.08.010.
26. Yuan, X., Yi, M., Dong, B., Chu, Q., and Wu, K. (2021). Prognostic significance of KRT19 in Lung Squamous Cancer. J. Cancer *12*, 1240–1248. https://doi.org/10.7150/jca.51179.
27. Saha, S.K., Kim, K., Yang, G.-M., Choi, H.Y., and Cho, S.-G. (2018). Cytokeratin 19 (KRT19) has a Role in the Reprogramming of Cancer Stem Cell-Like Cells to Less Aggressive and More Drug-Sensitive Cells. Int. J. Mol. Sci. *19*, 1423. https://doi.org/10.3390/ijms19051423.
28. Liu, J., Xiao, Q., Xiao, J., Niu, C., Li, Y., Zhang, X., Zhou, Z., Shu, G., and Yin, G. (2022). Wnt/β-catenin signalling: function, biological mechanisms, and therapeutic opportunities. Signal Transduct. Targeted Ther. *7*, 3. https://doi.org/10.1038/s41392-021-00762-6.
29. Russell, J.O., and Monga, S.P. (2018). Wnt/β-Catenin Signaling in Liver Development, Homeostasis, and Pathobiology. Annu. Rev. Pathol. *13*, 351–378. https://doi.org/10.1146/annurev-pathol-020117-044010.
30. Fu, Z., Chen, C., Zhou, Q., Wang, Y., Zhao, Y., Zhao, X., Li, W., Zheng, S., Ye, H., Wang, L., et al. (2017). LncRNA HOTTIP modulates cancer stem cell properties in human pancreatic cancer by regulating HOXA9. Cancer Lett. *410*, 68–81. https://doi.org/10.1016/j.canlet.2017.09.019.
31. Lee, Y.S., and Dutta, A. (2009). MicroRNAs in cancer. Annu. Rev. Pathol. *4*, 199–227. https://doi.org/10.1146/annurev.pathol.4.110807.092222.
32. Beveridge, D.J., Richardson, K.L., Epis, M.R., Brown, R.A.M., Stuart, L.M., Woo, A.J., and Leedman, P.J. (2021). The tumor suppressor miR-642a-5p targets Wilms Tumor 1 gene and cell-cycle progression in prostate cancer. Sci. Rep. *11*, 18003. https://doi.org/10.1038/s41598-021-97190-x.
33. Wang, X., Song, Z., Hu, B., Chen, Z., Chen, F., and Cao, C. (2021). MicroRNA-642a-5p inhibits colon cancer cell migration and invasion by targeting collagen type I α1. Oncol. Rep. *45*, 933–944. https://doi.org/10.3892/or.2020.7905.
34. Chen, X., Zeh, H.J., Kang, R., Kroemer, G., and Tang, D. (2021). Cell death in pancreatic cancer: from pathogenesis to therapy. Nature Reviews. Nat. Rev. Gastroenterol. Hepatol. *18*, 804–823. https://doi.org/10.1038/s41575-021-00486-6.
35. Xing, S., Tian, Z., Zheng, W., Yang, W., Du, N., Gu, Y., Yin, J., Liu, H., Jia, X., Huang, D., et al. (2021). Hypoxia downregulated miR-4521 suppresses gastric carcinoma progression through regulation of IGF2 and FOXM1. Mol. Cancer *20*, 9. https://doi.org/10.1186/s12943-020-01295-2.
36. Ma, L., Craig, A.J., and Heinrich, S. (2021). Hypoxia is a key regulator in liver cancer progression. J. Hepatol. *75*, 736–737. https://doi.org/10.1016/j.jhep.2021.05.032.
37. Lee, M. (2009). Hypoxia targeting gene expression for breast cancer gene therapy. Adv. Drug Deliv. Rev. *61*, 842–849. https://doi.org/10.1016/j.addr.2009.04.017.
38. DePeaux, K., and Delgoffe, G.M. (2021). Metabolic barriers to cancer immunotherapy. Nat. Rev. Immunol. *21*, 785–797. https://doi.org/10.1038/s41577-021-00541-y.
39. Yang, M.-H., Wu, M.-Z., Chiou, S.-H., Chen, P.-M., Chang, S.-Y., Liu, C.-J., Teng, S.-C., and Wu, K.-J. (2008). Direct regulation of TWIST by HIF-1alpha promotes metastasis. Nat. Cell Biol. *10*, 295–305. https://doi.org/10.1038/ncb1691.
40. Shukla, S.K., Purohit, V., Mehla, K., Gunda, V., Chaika, N.V., Vernucci, E., King, R.J., Abrego, J., Goode, G.D., Dasgupta, A., et al. (2017). MUC1 and HIF-1alpha Signaling Crosstalk Induces Anabolic Glucose Metabolism to Impart Gemcitabine Resistance to Pancreatic Cancer. Cancer Cell *32*, 71–87.e7. https://doi.org/10.1016/j.ccell.2017.06.004.
41. Lin, J., Wang, X., Zhai, S., Shi, M., Peng, C., Deng, X., Fu, D., Wang, J., and Shen, B. (2022). Hypoxia-induced exosomal circPDK1 promotes pancreatic cancer glycolysis via c-myc activation by modulating miR-628-3p/BPTF axis and degrading BIN1. J. Hematol. Oncol. *15*, 128. https://doi.org/10.1186/s13045-022-01348-7.
42. Chen, K., Wang, Q., Liu, X., Wang, F., Yang, Y., and Tian, X. (2022). Hypoxic pancreatic cancer derived exosomal miR-30b-5p promotes tumor angiogenesis by inhibiting GJA1 expression. Int. J. Biol. Sci. *18*, 1220–1237. https://doi.org/10.7150/ijbs.67675.

STAR★METHODS

KEY RESOURCES TABLE

REAGENT or RESOURCE	SOURCE	IDENTIFIER
Antibodies		
anti-KRT19 antibody	Proteintech	Cat# 14965-1-AP, RRID:AB_2133324
anti-Vimentin antibody	ServiceBio	Cat# GB111308, RRID:AB_3206250
anti-N-cadherin antibody	ServiceBio	Cat# GB111273, RRID:AB_3206251
anti-E-cadherin antibody	ServiceBio	Cat# GB11082, RRID:AB_3094439
anti-Cyclin D1 antibody	ServiceBio	Cat# GB111935, RRID:AB_3206252
anti-c-Myc antibody	ServiceBio	Cat# GB113748, RRID:AB_3206253
anti-β-catenin antibody	ServiceBio	Cat# GB12015, RRID:AB_3206254
anti-HIF1α antibody	ServiceBio	Cat# GB111339, RRID:AB_3206255
anti-GAPDH antibody	ServiceBio	Cat# GB12002, RRID:AB_3206256
anti-Ki67 antibody	ServiceBio	Cat# GB121141, RRID:AB_3083641
anti-KRT19 antibody	Thermo Fisher Scientific	Cat# PA5-118020, RRID:AB_2902624
anti-HIF1α antibody	Proteintech	Cat# 20960-1-AP, RRID:AB_10732601
HRP-conjugated Affinipure Goat Anti-Rabbit IgG	Proteintech	Cat# SA00001-2; RRID: AB_2722564
HRP-conjugated Affinipure Goat Anti-Mouse IgG	Proteintech	Cat# SA00001-1-A; RRID: AB_2890995
Bacterial and virus strains		
LV-sh-KRT19	GeneChem (Shanghai, China).	GIEL0334167
LV-oe-KRT19	GeneChem (Shanghai, China).	GOSL0376023
Biological samples		
Pancreatic cancer tissue specimen	The First Hospital of Lanzhou University	LDYYLL-2023-506
Chemicals, peptides, and recombinant proteins		
protease inhibitor	Servicebio	Cat# G2006
phosphatase inhibitor	Servicebio	Cat# G2007
PEI 40 K	Servicebio	Cat# G1802
Puromycin	Solarbio	Cat# *P8230*
XAV-939	TargetMol	Cat# T1878
Critical commercial assays		
TRIzol reagent	Takara	Cat# 9108
PrimeScript™ RT Reagent Kit	Takara	Cat# RR047A
TB Green Premix Ex Taq	Takara	Cat# RR820A
RIPA buffer	Boster	Cat# AR0102
BCA Protein Assay Kit	Boster	Cat# AR0146,
ECL	Servicebio	Cat# G2014
Cell Counting Kit-8	APExBIO	Cat# K1018
Annexin V-IF647/PI Cell Apoptosis Detection Kit	Servicebio	Cat# G1514
Dual-Luciferase Reporter Gene Assay Kit	Yeasen	Cat# 11402ES60
EdU test kit	Servicebio	Cat# G1602
Deposited data		
Raw and analyzed data	This paper	GEO: GSE15471, GSE16515

(*Continued on next page*)

Continued

REAGENT or RESOURCE	SOURCE	IDENTIFIER
Experimental models: Cell lines		
HPDE6-C7	Bena Culture Collection	BNCC 359453
BxPC-3	Chinese Academy of Science	TCHu 12
AsPC-1	Chinese Academy of Science	SCSP-5080
SW 1990	Chinese Academy of Science	TCHu201
PANC-1	Chinese Academy of Science	SCSP- 535
Experimental models: Organisms/strains		
Male BALB/c nude mice (4–6 weeks old)	Cavins (Changzhou, China)	LDYYLL-2023-506
Oligonucleotides		
siRNAs and miRNAs, please see Table S1	This paper	N/A
For primers, please see Table S2	This paper	N/A
Software and algorithms		
ImageJ software	National Institutes of Health	https://imagej.nih.gov/ij
GraphPad Prism 9.5	GraphPad Prism Software, Inc	https://www.graphpad.com/
SPSS 22.0 software	IBM corporation	https://www.ibm.com/spss

EXPERIMENTAL MODEL AND STUDY PARTICIPANT DETAILS

Patients with PC

Fifty-three pairs of PC and matched paracancerous tissues, along with relevant clinicopathological data, were obtained from patients who underwent surgical procedures between March 2018 and June 2022 at the First Hospital of Lanzhou University. Specimens were obtained from individuals with histologically confirmed primary PC who had not undergone chemotherapy or radiotherapy prior to surgery. The study received approval from the hospital's medical ethics committee (Number: LDYYLL-2023-506), and all participating patients provided informed consent. All tissues were immediately frozen at −80°C. All PC patients belong to the East Asian population (Han Chinese ethnic group in China), and their clinical and pathological characteristics are detailed in Table 1.

Cell culture

BxPC-3, AsPC-1, SW 1990, PANC-1, and human PC cell lines were acquired from the Chinese Academy of Science (Shanghai, China). We acquired the HPDE6-C7 normal human pancreatic ductal epithelial cell line from the Bena Culture Collection (Beijing, China). A short tandem repeat DNA analysis was performed to identify the cells. Subsequently, PANC-1 and SW 1990 cells were cultivated in Dulbecco's modified Eagle's medium (C11995500BT, Gibco), and RPMI 1640 medium (C11875500BT, Gibco) was used to cultivate BxPC-3, HPDE6-C7, and AsPC-1 cells. After adding 10% fetal bovine serum (FBS; AB-FBS-0500S, ABW) and 1% penicillin-streptomycin solution (G4003, Servicebio) to the medium, they were incubated at 37°C in a 5% CO_2 incubator. The cells were cultivated at 37°C in a hypoxia chamber with 1% oxygen and 5% CO_2 to induce hypoxic exposure.

Cell transfection

KRT19 knockdown or overexpression and negative control (NC) lentiviruses were acquired from GeneChem (Shanghai, China). Small interfering RNAs (siRNAs) specifically designed to target HIF1α, miR-642a-5p mimics, inhibitors, and their corresponding NCs were acquired from GenePharma (Shanghai, China). Additionally, AsPC-1 and BxPC-3 cells, intended for stable transfection, were introduced into 6-well plates at a concentration of approximately 40%–50%. Subsequently, 10 μL of lentivirus was added to each well. Infected cells were screened by adding 2 μg/mL puromycin (P8230, Solarbio) 48 h after transfection for 1 week. Transient transfection of all siRNAs, miRNA mimics, and inhibitors into cells using PEI 40 K (G1802, Servicebio) was performed according to the manufacturer's guidelines. In addition, 10 μmol/L of XAV-939 (HY-15147, MCE) was deployed to inhibit the WBC pathway. The transfection was verified by qRT-PCR or western blotting. Table S1 summarizes related siRNA sequences.

Animal experiments

Ten male BALB/c nude mice (4–6 weeks old) were procured from Cavins (Changzhou, China). Two sets of BxCP-3 cells (n = 5) were randomly assigned; BxCP-3 cells transduced with sh-*KRT19* or ctrl lentivirus (1×10^6) were dissolved in 150 μL of PBS and subsequently administered subcutaneously into the front armpit of mice. Tumor dimensions were assessed at 4-day intervals, and tumor volume was determined as follows: Volume = (length × width2)/2. The mice were euthanized 4 weeks after injection, and the tumors were excised, weighed, and imaged. A

portion of the tumor was excised for hematoxylin and eosin (H&E) and immunohistochemical staining, while the rest of the tumors were stored at −80°C. This animal trial was approved by the Ethics Review Committee of the First Hospital of Lanzhou University (number: LDYYLL-2023-506).

METHOD DETAILS

Quantitative reverse transcriptase polymerase chain reaction (qRT-PCR)

Total RNA was extracted from cells and tissues using the TRIzol reagent (9108, Takara), followed by reverse transcription using the PrimeScript RT Reagent Kit (RR047A, Takara). TB Green Premix Ex Taq (RR820A, Takara) was used to perform qPCR on a real-time PCR detection system (BioRad, CFX96). The data were measured using the $2^{-\Delta\Delta Ct}$ technique. Expression was normalized using either U6 or GAPDH as endogenous controls. The primer sequences used are presented in Table S2.

Western blotting

Total protein was extracted from the cells or tissues using RIPA buffer (AR0102, Boster) containing a protease inhibitor mixture (G2006, Servicebio) and a phosphatase inhibitor (G2007, Servicebio). The protein content was determined using a BCA Protein Assay Kit (AR0146, Boster). Subsequently, 40 μg of protein was divided and placed on either a 10% or 6% SDS-PAGE gel and deposited onto PVDF membranes (G6044, Servicebio). Following a 2-h blocking step using skim milk powder (GC310001, Servicebio), the membranes underwent an overnight treatment at 4°C with the appropriate primary antibodies and were exposed to secondary antibodies and left to incubate for 1 h at room temperature. The specific primary antibodies employed were: KRT19 (1:500, 14965-1-AP, Proteintech), Vimentin (1:1000, GB111308, Servicebio), N-cadherin (1:1000, GB111273, Servicebio), E-cadherin (1:1000, GB11082, Servicebio), cyclin D1 (1:1000, GB111935, Servicebio), c-Myc (1:1000, GB113748, Servicebio), β-catenin (1:1000, GB12015, Servicebio), hypoxia-inducible factor 1 alpha (HIF1α) (1:1000, GB111339, Servicebio), and GAPDH (1:1000, GB12002, Servicebio). Protein expression was detected using an ECL western blotting substrate (G2014, Servicebio), and the membranes were imaged using a membrane imaging device (Clinx, ChemiScope S6).

Cell counting Kit-8 (CCK-8) experiments

The CCK-8 test (K1018, APExBIO) included the transfection of transfected cells onto 96-well plates with a density of 2,000 cells in 100 μL of media per well. Subsequent to inoculation, 10 μL of CCK-8 reagent was introduced at 0, 24, 48, and 72 h, and the cells were incubated at 37°C for 2 h. Cell viability was assessed using a plate reader (BioTek, Synergy H1) by determining the absorbance at 450 nm.

Wound healing (WH) assay

PC cells were seeded in 6-well plates. The cell monolayer was scratched with a 200 μL pipette tip once the cell density reached around 90%. The suspended cells were washed with phosphate-buffered saline (PBS) and cultured in a medium containing 1% FBS. WH was captured using an inversion microscope at 0 and 24 h. Cell migration was examined using the ImageJ software.

Transwell assays

PC cells were initially deprived of serum in the medium for 12 h and quantified to a concentration of 2 × 105 cells/mL by trypsinized digestion (G4001, Servicebio). The cells were introduced into the upper transwell chamber (TCS003024, BIOFIL) using 200 μL of serum-free media. For invasion and migration tests, a matrix gel (356234, Corning) was added. The bottom chambers were supplemented with 700 μL of media enriching 20% FBS. Following the incubation of the culture plates for 24 h, the cells were fixed with 4% paraformaldehyde (G1101, Servicebio) for 30 min and then exposed to 0.1% crystal violet (G1062, Solarbio) for an additional 30 min. Migrated and invaded cells were observed under a microscope.

Flow cytometry

To detect apoptosis, we first collected PC cell culture supernatants and subsequently digested the collected PC cells with ethylenediaminetetraacetic acid-free trypsin (G4002, Servicebio), followed by washing twice with PBS pre-cooled at 4°C. Subsequently, cell staining was performed using a flow cytometric apoptosis kit (G1514, Servicebio) following the manufacturer's protocols. A flow cytometer (Agilent, NovoCyte Advanteon Dx VBR) was used to perform flow cytometry with software.

Luciferase reporter assay

The KRT19 3′-UTR luciferase reporter vectors, both wild-type (WT) and mutant (MUT) were obtained from Genecreate (Wuhan, China). The HEK-293 T cells were seeded into 24-well plates. Subsequently, WT and MUT reporter vectors, together with the miR-642a-5p overexpression vector, were co-transfected into 293 T cells employing Lipofectamine 2000 (11668019; Invitrogen). Firefly and *Renilla* luciferase activity levels were assessed following a 48-h incubation period using the Dual-Luciferase Reporter Gene Assay Kit (11402ES60, Yeasen). *Renilla* luciferase activity was used to standardize transfection effectiveness.

Immunohistochemistry

The excised tumor tissues were sliced into 4 μm sections to prepare slides. The slides were deparaffinized with xylene and rehydrated using ethanol. Some of the slices were stained with H&E, while others were subjected to further experiments. Following incubation with a 3% hydrogen peroxide solution to inhibit naturally occurring peroxidase activity and restore the antigen, the sections were submerged in sodium citrate buffer. To prevent binding to nonspecific sites, a 3% BSA solution (GC305010, Servicebio) was introduced. The sections were exposed to anti-Ki67 (1: 1000, GB121141, Servicebio) and anti-KRT19 (1: 2000, 14965-1-AP, Proteintech) primary antibodies at 4°C overnight, followed by exposure to secondary antibodies. The images were scanned with a digital slide scanner (3DHISTECH, Pannoramic 250FLASH) and analyzed using Caseviewer 2.4 software (3DHISTECH).

5-Ethynyl-2′-deoxyuridine (EdU) experiment

The PC cells were distributed evenly at a consistent density in a 24-well plate. Following attachment to the cell wall, cell proliferation was determined using an EdU test kit (G1602, Servicebio) according to the manufacturer's instructions. The cells were then treated with 4% paraformaldehyde for 15 min and rinsed three times with PBS. Cells were cleared using 1% Triton (GC204003, Servicebio) for 15 min. A fluorescence microscope (Olympus, IX73) was used to capture images. Cell counting was conducted in three randomly selected areas, and the cell proliferation rate was calculated by dividing the cell number labeled with EdU by the total cell number.

Co-immunoprecipitation (CoIP) assay

AsPC-1 and BxPC-3 cells cultivated under low-oxygen conditions (hypoxia) or normal-oxygen conditions (normoxia) were treated with IP lysate (G2038, Servicebio) to extract cellular components. The extracted components were incubated with either normal IgG, anti-KRT19 (1:1000, PA5-118020, Thermo Fisher Scientific), or anti-HIF1α (1:1000, 20960-1-AP, Proteintech) antibodies. The incubation was conducted on a rotator at 4°C overnight. The AB–protein complexes were collected through incubation with protein A/G beads (IP05, Millipore) for 2 h, and the complexes were examined using western blotting.

Bioinformatics analysis

Gene expression profiles from GSE15471 (39 non-tumorous and 39 PC samples; platform: GPL570) and GSE16515 (36 PC and 16 non-tumorous samples; platform: GPL570) were acquired using the Gene Expression Omnibus (http://www.ncbi.nlm.nih.gov/geo/). We merged two microarrays comprising 75 PC and 55 control specimens. Furthermore, we used R 4.2.1 software to screen for differentially expressed mRNA (|LogFC| > 2 and p.adj <0.05) and discovered 182 differentially expressed genes (DEGs), which were used to create a heatmap using the ComplexHeatmap package. The clusterProfiler R package was used to perform gene set enrichment analysis (GSEA) of relevant signaling pathways. Immunohistochemistry (IHC) staining for KRT19 in PC was performed using the Human Protein Atlas (HPA; https://www.proteinatlas.org/). The Gene Expression Profiling Interactive Analysis (GEPIA) database (http://gepia.cancer-pku.cn/) was accessed to analyze *KRT19* expression and prognosis in PC and investigate the correlation between HIF1α and *KRT19* in PC. TargetScan (http://www.targetscan.org/), miRWalk (http://mirwalk.umm.uni-heidelberg.de/), and StarBase (https://starbase.sysu.edu) were used. Online databases were used to predict the miRNAs that can regulate *KRT19*. The StarBase database was used to analyze miR-642a-5p expression and prognosis in PC and its correlation with KRT19.

QUANTIFICATION AND STATISTICAL ANALYSIS

Statistical analysis was conducted using GraphPad Prism 9.5 and SPSS 22.0 software. Data are reported as the mean ± standard deviation. Data from two groups were compared using the Student's t-test, while variations between several groups were evaluated using a one-way analysis of variance. Additionally, we used the chi-square test to examine the correlation between KRT19 expression and the clinicopathological characteristics of patients in 53 pairs of PC samples. Spearman's rank correlation analysis was used to examine bivariate correlations between variables. P-values are represented by asterisks (*) in the graphs (*$p < 0.05$, **$p < 0.01$, ***$p < 0.001$, and ****$p < 0.0001$).